

Trends and shifts in time series of climate data generated by GCM from 2006 to 2090

M. L. SANE^{1*}, S. SAMBOU¹, S. DIATTA², I. LEYE¹, D. M. NDIONE¹, S. SAUVAGE³, J.M. SANCHEZ-PEREZ³, S. KANE¹,

¹*Faculty of Sciences and Technics. Department of Physics. Cheikh Anta Diop University. Dakar. Senegal*

²*UFR Science and Technology - Dept of Physics. University of Assane Seck. Ziguinchor*

³*EcoLab, University of Toulouse, CNRS, INPT, UPS, Avenue de l'Agrobiopole, 31326 Castanet-Tolosan, France;*

mousselanding.sane@ucad.edu.sn

Keywords: Senegal River, Bafing River, GCM, SWAT, Climate Change

----- ◆ -----

Abstract

Like many African countries, Senegal faces significant challenges in water resources management due to high variability of annual floods, and climate change effects. As attenuation measures, Diama and Manantali Hydrosystem has been built on the Senegal river basin, the first to stop sea water intrusion, the second as multipurpose one for irrigation, energy supply among others. It becomes by the way very important to assess the effect of climate change on water resources management of the Manantali Dam. The semi-distributed model SWAT has been first calibrated and validated on the Bafing River basin. Outputs of Three models of General Circulation Mode (CCCmaCanESM2; MOHC-HadGEM2-ES MPI-M-MPI-ESM-LR) has been used as input to SWAT to generate daily flows at Bafing Makana stream gauge for the period 2006-2090. Statistical tool Khronostat are used to test the obtained time series of annual flows for shift and trends for each scenario. For higher scenario, upwards trends and increasing shifts have been noted for annual flows, while.

1. INTRODUCTION

The challenges of 21st century is food security, fight against poverty and climate change. Climate change is one of the biggest challenges that human societies face nowadays [1]. A comprehensive review of the potential impacts of climate change indicates that runoff, precipitation and temperatures are probably going to increase

by the end of the 21st century [2], [3]. The climate global changing will have a range of significant impacts, including on extreme weather events, natural ecosystems, human's health and economic activity [4]. The Climate is characterized in Africa by a wide variety of climate systems ranging from humid equatorial, through seasonally-arid tropical, to sub-tropical Mediterranean-type climates [5]. The countries of West

Africa are among the most vulnerable to impacts of climate change [6].

The Senegal river is the second most important river of West Africa, after the Niger [7]. In 1960, a reduction of flow near 60% was detected due to the climate change on Senegal River [8], [9]. This led to the creation in 1972 of the Organization for the Development of the Senegal River (OMVS). Its major concern was to develop infrastructure to address water stress resulting from a cycle of droughts, develop agriculture, reduce the cost of hydro-electricity and open up Mali by improving navigation. The economic and social activities of this river are closely linked to the availability of water resources. The most important economic sectors are agriculture and energy production. A Manantali dam is built on Bafing River and was made has been commissioned in 1988 and controls about 40 to 60% of the Senegal River flows. This dam is multipurpose (Hydropower, irrigation, low water and flood support). Knowledge of flow behavior on Bafing River is very important for management of water resource of Manantali dam. In 1990 Senegal river advantage of the upturn of the flows [10]. Statistical test is used to know flow behavior. There are several statistical tools to detect trends and shifts in hydrological time series (precipitation, temperature and flow). Similarly, to appreciate impact of climate change, the global climate models are used. The methods and techniques developed for detecting shifts in hydrological time series and description of different approaches involved in adjusting climate data have been investigated by many researchers [11],

[12], [13]. Tests for significant trends detection in climatologic time series can be classified as parametric or non-parametric methods. Parametric trend tests require data to be both independent and normally distributed, while non-parametric trend tests require only that the data be independent [14]. The statistical tests have been applied to study the comportment of precipitation, temperature and flows using is observed or generated. [15] applies Pettitt method to assess change point of flow on two gauges stations of the Yangtze River of China during the period 1882-2010. [16] use Mann-Kendall test, Modified Mann-Kendall and Sen's slope estimator to determinate trends of monthly variability of rainfall, from 1971 to 2010. [17] applies Mann-Kendall test to put in evidence trend in the available series of annual maximum and minimum temperature for the study area for a period of 1901- 2007. Mann-Kendall test and Sen's Slope Estimator have been applied in Jakara River Basin at the period 2001-2010 by [18] to detect and quantify trend in the precipitation and water quality time series. In Senegal, [11] assess the climate variability and change in annual and monthly data rainfall behavior between 1970 and 2010 through statistical tests for trends, shift and randomness. [19] applied Standardized Precipitation Index, Climatic Moisture Index and Hubert's Procedure of Segmentation to assess drought in Senegal River. This study shows that the reduction of rainfall at 1970, 1980 and 1990 decades. HBV model has been calibrated, validated Richmond River Catchment and forced on with seven Global Climate Model to evaluate impacts of future climate change

on the hydrological response [20]. The results of this study show that the hydrological status of the catchment is likely to change significantly.

The main objective of the present work is to check for trends and shifts in the time series of flow in the Bafing River Catchment (Senegal River) at the Bafing Makana stream gauge. The CMIP5 project climate models are used in these studies. They allow to assess the projected changes in future rainfall under four different greenhouse gas emission scenarios called RCPs (Representative Concentration Pathways). The fourth generation of GCM simulations from Canadian Centre for Climate Modelling and Analysis are used in this paper to generate climate data: CCCmaCanESM2, with resolution $\sim 2.8^\circ$,

2. Material and methods

2.1. Study Area

The study area is the watershed of Bafing River upstream of the Bafing Makana stream gauge (figure 1). It is located between $10^\circ 30'$ and $12^\circ 30'$ north latitude and between $12^\circ 30'$ and $9^\circ 30'$ west longitude. Bafing Makana is the main tributary of Senegal River. The Senegal River is a transboundary River. It crosses Guinea, Mali Mauritania and Senegal. This Basin Development Organization (OMVS) is a regional cooperative management body of the Senegal River which currently includes Guinea,

Met Office Hadley Centre England (MOHC-HadGEM2-ES) and Max Planck Institute for Meteorology (MPI-M-MPI-ESM-LR).

Two RCPs scenario of green gas emission have been selected for analysis: RCP45 representing the mid-range greenhouse gas emission scenarios and the RCP85 representing the high-end greenhouse gas emission scenarios corresponding to a 'worst case scenario'. Outputs climate data of these scenario have been used as inputs to SWAT model to generate time series of flows at Bafing Makana stream gauge for the period 2006-2090. Mann-Kendall and Sen's slope trend test detection and Hubert's procedure and Pettitt change point analysis test have been used.

Mali, Mauritania, and Senegal. Senegal River upstream Bafing Makana has a tropical climate with annual mean temperature is 27.6°C annual mean rainfall of 1166 mm (Climate-Data.org). Four fictitious rain gauge station of the Bafing River Basin are selected (Table 1).

Table 1: Rain gauges stations coordinates

Station Fictitious	Latitude	Longitude	Location
S0	13.19°	-10.42°	Outlet of Manantali Dam
S1	12.12°	-10.48°	Near Bafing Makana
S2	11.51°	-10.78°	Upstream Dakka Saidou
S3	11.22°	-11.34°	South of Bafing river

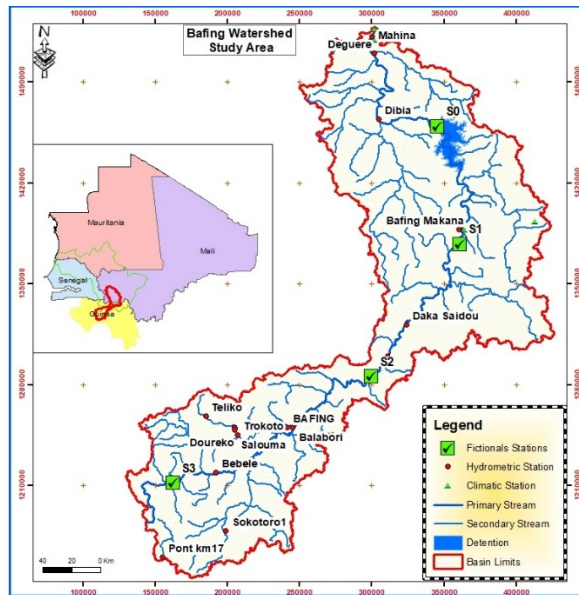


Figure 1: Bafing River Catchment

2.2. Tools and Data using

SWAT (Soils Water Assessment Tools), a physically based hydrologic model, has been selected as rainfall runoff model to generate flow. SWAT model inputs are topography, land-use, soil, climatic data, and stream flow data. It gives as stream flows as outputs. Topography was defined by a digital elevation model (DEM). SWAT model can use one or many gauges station located in study area. SWAT model was calibrated and validated on Bafing River. Statistical treatment has been performed using Khronostat 10.1. Khronostat is a tool for processing data developed by IRD. It allows to put out shifts in time series.

2.3. Description of Global Circulation Model (GCM)

Global Climate Models are mathematical tools based on equations of fundamental physics. They are able to simulate many important aspects of Earth's climate [21] (Hayhoe et al., 2017): large-scale patterns of temperature and precipitation, general

characteristics of storm tracks and extratropical cyclones, and observed changes in global mean temperature and ocean heat content as a result of human emissions. Forecasts of changes in future climate due to emissions from human activities begin with the development of emission scenarios. These scenarios are not predictions, but represent plausible future conditions under particular assumptions. The emission scenarios were developed in the mid-1990s and are based on 4 different storylines (Figure 2). Each storyline represents different world futures [22], [23], [8].

- a world with quick economic growth and a quick launch of new and efficient technologies (A1),
- a very heterogenic world with focus on family values and local traditions (A2),
- a world without materialism and launch of clean technologies (B1)
- a world with focus on local solutions for economic and ecological sustainability (B2)

Climate models are the main tools for investigating projected long-term precipitation changes. These models can be applied in two cases: simulate past precipitation and simulate possible future precipitation under different greenhouse gas emission scenarios [24]. Climate models has allowed to replicate long-term climatological changes in observed precipitation with considerable success [3]. The general circulations models used in this paper are Canadian Centre for Climate Modelling and Analysis (CCCma-

CanESM2), Met Office Hadley Centre. England (MOHC-HadGEM2-ES) and Max Planck Institute for Meteorology (MPI-M-MPI-ESM-LR) and were identified in literature [25], [26], [26], [28]. Two emissions scenarios medium (RCP4.5) and high (RCP8.5) have been associated to all these models. In the table 2 we present the characteristics of the climate model used in this paper.

Table 2: Main characteristics of the considered CMIP5 models

Model	Modeling Center	Type of GCM	Horizontal resolution (lat/lon)
CanESM2	CCCma (Canada)	ESM	2.8° / 2.8°
HadGEM2-ES	MOHC (UK)	ESM	1.25° / 1.875°
MPI-ESM-LR	MPI-M (Germany)	ESM	1.9° / 1.875°

The climatic input data are generated from climate models. They consist of rainfall, temperature, relative humidity, solar radiation and wind speed. The Rainfall and temperature were presented in table 3 on the period of study, 2006-2090. The rainfall means annual increase from Northern to Southern and the temperature decrease from Southern to Northern.

Table 3: Rainfall and temperature data on the period of study

CCCma-CanESM2						
	Rainfall mm		Tmax mean		Tmin mean	
	Rcp4.5	Rcp8.5	Rcp4.5	Rcp8.5	Rcp4.5	Rcp8.5
S0	723	711	23.3	38.7	22.2	37.8
S1	1259	1242	21.9	37.4	20.8	36.5
S2	1340	1349	21.0	35.8	19.9	35.0
S3	3657	3612	19.6	32.4	18.7	31.6
MOHC-HadGEM2-ES						
	Rainfall		Tmax mean		Tmin mean	
	Rcp4.5	Rcp8.5	Rcp4.5	Rcp8.5	Rcp4.5	Rcp8.5
S0	980.1	1015	36.5	37.4	22.1	23.2
S1	1575	1650	35.2	36	20.7	21.8
S2	1582	1659	33.7	34.5	19.8	20.9
S3	3925	4136	30.3	31.1	18.5	19.5
MPI-M-MPI-ESM-LR						
	Rainfall		Tmax mean		Tmin mean	
	Rcp4.5	Rcp8.5	Rcp4.5	Rcp8.5	Rcp4.5	Rcp8.5
S0	1127	1152	35.8	36.6	21.2	22.2
S1	1670	1736	34.5	35.3	19.9	20.8
S2	1669	1738	33.0	33.8	19.0	19.9
S3	4036	4150	29.8	30.5	18.0	18.8

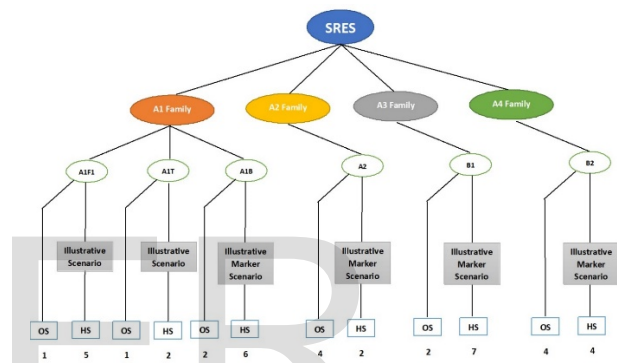


Figure 2: Schematic illustration of SRES scenarios. Four qualitative storylines yield four sets of scenarios called “families”: (Source: IPCC, 2000)

2.4. Description of the Statistic Tools

Statistical analysis is fundamental to all study of climates data. It is the main tool used in time series analysis

2.4.1. Shifts Test

Detection of abrupt shift in long time series of hydrological data is gaining in interest since researches an important and difficult issue, of increasing interest. In this study we use Hubert procedure of segmentation of time series and Pettitt test. The null hypothesis H_0 is “no shift in the time series” and the significance level is of $\alpha = 0.05$. A

brief description of these of these tests is presented below.

- Hubert Procedure of Segmentation [29]

In the Hubert procedure of segmentation, the time series is divided into m consecutive segments. The mean values calculated on the segment can be significantly different to the mean of the raw data [10]. The method searches the multiple change of means in the time series. The null hypothesis is accepted if the process of segmentation is order three or plus segments. The segmentation is defined by:

- Pettitt Test [30]

The Pettitt test is a rank-based nonparametric statistical test. It detects a significant change in the mean of a time series when the exact date of the change is unknown. This test is extensively employed in both hydrological and precipitation shift detection studies. The null hypothesis H_0 is “no shift in the time series”, while the alternative hypothesis H_1 is “an upward or downward shift. H_0 is tested at the 5% significance level [31]. The null hypothesis of the test is that, when arbitrarily splitting the sample in two segments, there is no change in the mean value of each segment [15]. To achieve the identification of change point, a statistical index $U_{t,N}$ is defined as follows.

$$U_{t,N} = \sum_i^t \sum_{j=t+1}^N D_{ij} \quad (1)$$

$$D_{i,j} = \text{sgn}(x_i - x_j) \begin{cases} 1 \text{ if } (x_j - x_i) > 0 \\ 0 \text{ if } (x_j - x_i) = 0 \\ -1 \text{ if } (x_j - x_i) < 0 \end{cases} \quad (2)$$

Given a certain significance level α , if the p-value $p < \alpha$, the null hypothesis is rejected and the time series present a significant change point for the level α .

2.4.2. Trends Tests

The trends and variability in hydrological variables are assessed using a statistical test for trend as well as further data analysis to examine the relationship between hydrological variables and climatic factors [32]. We chose therefore to use a nonparametric test (Mann Kendall test) to detect the presence of a trend, a nonparametric estimate of the slope of the trend (Sen's slope estimate).

- Mann-Kendall test

The non-parametric Mann-Kendall test has been used to assess the presence of significant trends in flows data. It determines if a monotonic increasing or decreasing long-term trend exists. The Mann Kendall test have been used in earlier studies to detect trend in rainfall data [33]. Test statistic S of the test is defined as follows:

$$S = \sum_{i=1}^{n-1} \sum_{j=i+1}^n \text{sgn}(x_j - x_i) \quad (3)$$

where x_1, x_2, \dots, x_n represent n data point and x_j represents the data points at time j .

$$\text{sgn}(x_j - x_i) = \begin{cases} 1 \text{ if } (x_j - x_i) > 0 \\ 0 \text{ if } (x_j - x_i) = 0 \\ -1 \text{ if } (x_j - x_i) < 0 \end{cases} \quad (4)$$

The test statistic (S) is assumed to be approximately normal, with $E(S) = 0$ for sample size $n \geq 8$ and with a variance given by equation (5)

$$Var(S) = \frac{n(n-1)(2n+5)}{18} \quad (5)$$

The standardized test statistic Z is computed by

$$Z_{MK} = \begin{cases} \frac{S-1}{\sqrt{Var(S)}} & \text{when } S > 0 \\ 0 & \text{when } S = 0 \\ \frac{S+1}{\sqrt{Var(S)}} & \text{when } S < 0 \end{cases} \quad (6)$$

The null hypothesis of no trend (increasing or decreasing) is rejected when $|Z_{MK}| > 1.96$. A positive or negative value of Z indicates an upward or downward trend, respectively [34].

- Sen's slope estimator

In the case a linear trend exists, the true slope can also be estimated by a nonparametric procedure developed by Sen [1968], which is closely linked to the Mann-Kendall test. This means that linear model $f(t)$ can be described as following:

$$f(t) = Qt + B \quad (7)$$

where Q is the slope B is a constant.

The slope estimates of N pairs of data are first computed by [35] (Tabari et al., 2015).

$$Q_i = \frac{x_j - x_k}{j - k} \quad (8)$$

where x_j and x_k are data values at time j and k respectively and $j > k$. The Sen's estimator of the slope is the median of these N values of Q_i . The N values of Q_i are ranked from the smallest to the largest [36].

The Sen's estimator is computed by:

$$Q_{ms} = Q\left(\frac{N+1}{2}\right); \text{ if N is odd} \quad (9)$$

$$Q_{ms} = \frac{1}{2} \left[Q\left(\frac{N}{2}\right) + Q\left(\frac{N+2}{2}\right) \right]; \text{ if N is even} \quad (10)$$

$$C_\alpha = Z_{1-\frac{\alpha}{2}} * \sqrt{Var(S)} \quad (11)$$

where Q_{ms} is the median slope; C_α is a standardized Gaussian statistic.

If the median slope is within the range of $\left(\frac{(n-C_\alpha)}{2}\right)$ and $\left(\frac{(n+C_\alpha)}{2}\right)$ the null hypothesis is accepted [11].

3. Results

3.1. Exploratory Data Analysis

In the figure 3 we compare the plots of observed and simulated flows versus time for rcp4.5 and rcp8.5 scenarios on the period 2006-2015. For station S0, S1 and S2 the flows observed are significantly higher than flows simulated for all models. However, at the station S3 the flow simulated are more important than the flow observed. This differences in flow is partly due to the difference of rain. It appears that the stream flow simulated from MPI-M-MPI+ESM-LR model is closer to observed stream values among all other climate models.



Figure 3: Comparison of flows observed and simulated for each gauge's station

In the table 4 we compare the mean of difference between observed flows and simulated flows. A positive value of this criteria corresponds to underestimation and a negative value to an overestimation. According to table 4, SWAT model underestimate the flows when climate data of rain gauge stations S0, S1 and S2 are used as inputs, and overestimate the flow when climate data of rain gauge S3 are used as inputs.

Table 4: Calculate mean of error (Using only one station)

	CCCma-CanESM2		MOHC-HadGEM2-ES		MPI-M-MPI+ESM-LR		Stations
	RCP8.5	RCP4.5	RCP8.5	RCP4.5	RCP8.5	RCP4.5	
$\frac{1}{N} \sum_{N=1}^{10} (Q_{obs} - Q_{sim})$	Q(m³/s)	Q(m³/s)	Q(m³/s)	Q(m³/s)	Q(m³/s)	Q(m³/s)	
	+211	+208	+202	+194	+157	+168	S0
	+151	+150	+147	+194	+93	+107	S1
	+155	+152	+147	+131	+116	+109	S2
	-271	-257	-176	-837	-280	-322	S3

+ : The Model underestimates the flows ; - :
The Model overestimates the flows

We use climate models (CCCma-CanESM2, MOHC-HadGEM2-ES MPI-M-MPI+ESM-LR), to generate climate data at rain gauge S1, S2 and S3. The data of association of rain gauges S1-2-3, S1-2, S1-3 and S2-3 are used as inputs by SWAT model to calculate stream flows at Bafing Makana stream gauges for the period 2006-2015. The calculated and observed values are plotted in Fig 4a) for S1-2-3, Fig 4b) for S1-2, Fig 4c) for S1-3 and Fig 4d) for S2-3. The objective is to test for the best climate model to be used in the Bafing River Basin upstream Bafing Makana.



Figure 4: Comparison of flows observed and simulated for combination gauge station

This result is corroborated by the table 5, where the mean of errors between simulated flows using each of these combinations of stations data (S1-2-3; S1-2, S1-3, S2-3) as inputs in SWAT model are compared to observed flows. According to the mean error criteria, it appears that the RCP4.5 medium scenario fits better the observed values for the CCCma-CanESM2 and the MOHC-HadGEM2-ES model. It appears that the RCP8.5 high scenario fits better the observed values for the MPI-M-MPI+ESM-LR.

Table 5: Calculate mean of error (Using combination of station)

	CCCma-CanESM2		MOHC-HadGEM2-ES		MPI-M-MPI+ESM-LR		
	RCP8.5	RCP4.5	RCP8.5	RCP4.5	RCP8.5	RCP4.5	Stations
$\frac{1}{N} \sum_{N=1}^{10} (Q_{obs} - Q_{sim})$	-117	-200	-11	-74	-36	-67	S1-2-3
	154	157	148	158	+114	+111	S1-2
	-67	-56	-337	-25	-99	-106	S1-3
	-28	-19	128	10	-52	-67	S2-3

+ : The Model underestimates the flows ; - : The Model overestimates the flows

We present in the table 6 the statistical characteristics of time series of mean annual flows for the period 2006-2090. For all climate models and for all scenarios, mean annual flow generated by Swat using climate data from S0, S1, S2 and S3 climate station increases from North to South according to the geographical location of these stations. The coefficient of variations for all stations and models vary between 0.1 and 0.2.

Table 6: Statistical characteristic of annuals flows time series

		CCCma-CanESM2			MOHC-HadGEM2-ES			MPI-M-MPI+ESM-LR		
		Period 2006-2090			Period 2006-2090			Period 2006-2090		
Scenario	Stations	Mean	SD	RD	Mean	SD	RD	Mean	SD	RD
(rcp4.5)	S0	43	12	0.3	55	21	0.4	47	25	0.5
	S1	104	28	0.3	117	43	0.4	79	36	0.5
	S2	103	29	0.3	117	43	0.4	78	28	0.4
	S3	534	131	0.2	508	137	0.3	367	75	0.2
(rcp8.5)	S0	47	9	0.2	60	23	0.4	106	26	0.2
	S1	112	22	0.2	60	24	0.4	170	38	0.2
	S2	120	20	0.2	130	50	0.4	158	26	0.2
	S3	548	59	0.1	1090	233	0.2	665	87	0.1

SD : Standard Deviation ; RD : Relative Deviation

3.2. Statistical Test for shift

In the table 7, 8, 9 and 10 we present the results of application of Pettitt method and Hubert's segmentation for the three models.

3.2.1. Pettitt Test

Results of Pettitt test on annual flow between 2006-2090 are presented in the table 7 (for stations S0, S1 S2 and S3 separately) and in table 8 (for combination S1-2-3, S1-2, S1-3 and S2-3) for all models and all scenario.

When stations are considered separately (table 7), the null hypothesis of no shift in time series is rejected for all models, for all scenarios and for all climate stations except station S0 for CCCma-CanESM2 model and station S3 for MOHC-HadGEM2-ES model. For the medium scenario (RCP4.5), occurs around year 2073 CCCma-CanESM2 model, 2042 for MOHC-HadGEM2-ES model and 2016 MPI-M-MPI+ESM-LR model. For scenario high (RCP8.5), the shift appears between years 2040 and 2055.

Table 7: Pettitt Test

Stations	CCCma-CanESM2		MOHC-HadGEM2-ES		MPI-M-MPI+ESM-LR		
	H ₀	<u>Year</u>	H ₀	<u>Year</u>	H ₀	<u>Year</u>	Scénario
S0	R	2073	R	2042	R	2016	RCP4.5
S1	R	2073	R	2042	R	2016	
S2	R	2073	R	2042	R	2016	
S3	R	2072	R	2035	R	2026	
S0	A	No Shift	R	2040	R	2046	RCP8.5
S1	R	2055	R	2040	R	2046	
S2	R	2040	R	2040	R	2046	
S3	R	2055	A	No Shift	R	2045	

R= H₀ « Rejected »; A= H₀ « Accepted »

When stations are considered combination (table 8), the null hypothesis of no shift in time series is rejected for all models, for all scenarios and for all climate stations except station S1-3 for MOHC-HadGEM2-ES model. For the medium scenario (rcp4.5), occurs around year 2073 CCCma-CanESM2 model, 2035 for MOHC-HadGEM2-ES model and 2028 MPI-M-MPI+ESM-LR model. For scenario high (rcp8.5), the shift appears between years 2040 and 2055.

Table 8: Pettitt Test (Using combination of stations)

	CCCma-CanESM2		MOHC-HadGEM2-ES		MPI-M-MPI-ESM-LR		
Stations	H ₀	Year	H ₀	Year	H ₀	Year	Scenario
S1-2-3	R	2074	R	2032	R	2028	RCP4.5
S1-2	R	2073	R	2042	R	2016	
S1-3	R	2072	R	2035	R	2028	
S2-3	R	2072	R	2035	R	2028	
S1-2-3	R	2055	R	2040	R	2040	RCP8.5
S1-2	R	2055	R	2040	R	2040	
S1-3	R	2055	A	No Shift	R	2045	
S2-3	R	2055	R	2040	R	2045	

R= H₀ « Rejected »; A= H₀ « Accepted »

3.2.2. Hubert's Procedure of Segmentation

The results for CCCmaCanESM2 model, MOHC-HadGEM2-ES model and MPI-M-MPI+ESM-LR model are presented respectively in tables 9, 10 and 11 with climate station S0, S1, S2, and S3 taken

separately. The medium and high scenario are considered.

The medium scenario (RCP4.5) indicates a downwards shift (50%) in time series of mean annual flow for all stations and for CCCmaCanESM2 and MPI-M-MPI+ESM-LR model (table 9 and 11). This scenario leads to an upwards shift (70%) for MOHC-HadGEM2-ES model (table 10).

For the high scenario (RCP8.5), an upwards shift occurs in flow time series of all station for all climate models and for all gauges stations. It's magnitude varies between 12 and 40%.

For the medium scenario, shifts are observed year 2073 (table 9), 2035 for (table 10) and 2015 (table 11). For scenario high, the shift appears between years 2039 and 2055.

Table 9: Results of two order Hubert's procedure for CCCmaCanESM2 model

CCCmaCanESM2										
	RCP4.5					RCP8.5				
Station			Mean	Decreases/ increases	Standard deviation			Mean	Decreases/ increases	Standard deviation
S0	2006	2073	47		9	No shift				
	2074	2090	25	-47	9					
S1	2006	2073	114		19	2006	2055	108		19
	2074	2090	59	-48	17	2056	2090	122	12	17
S2	2006	2073	115		17	2006	2055	331		28
	2074	2090	51	-56	9	2056	2090	378	14	30
S3	2006	2073	311		18	2006	2055	524		56
	2074	2090	149	-52	23	2056	2090	584	12	43

Table 10: Results of two order Hubert's procedure for MOHC-HadGEM2-ES model

MOHC-HadGEM2-ES										
	RCP4.5					RCP8.5				
Station			Me an	Decreases/ increases	Standard deviation			Mean	Decreases/ increases	Standard deviation
S0	2006	2037	39		16	2006	2039	43		21
	2038	2090	65	69	17	2040	2090	71	66	18
S1	2006	2042	82		29	2006	2040	45		23
	2043	2090	144	76	30	2041	2090	71	57	18
S2	2006	2042	82		29	2006	2039	87		36
	2043	2090	144	76	30	2040	2090	160	82	34
S3	2006	2035	373		93	2006	2006	1798		0
	2036	2090	583	56	92	2007	2090	1082	-40	221

Table 11: Results of two order Hubert's procedure for MPI-M-MPI-ESM-LR model

MPI-M-MPI-ESM-LR										
	RCP4.5					RCP8.5				
<u>tation</u>			Me an	Decreases/ increases	Standard deviation			Mean	Decreases/ increases	Standard deviation
S0	2006	2016	92		20	2006	2046	100		24
	2016	2090	40	-57	14	2048	2090	113	13	18
S1	2006	2015	162		23	2006	2024	158		28
	2016	2090	68	-58	18	2045	2090	192	22	25
S2	2006	2015	139		24	2006	2040	144		24
	2016	2090	69	-50	15	2041	2090	174	21	198
S3	2006	2015	536		55	2006	2045	621		51
	2016	2090	344	-36	39	2046	2090	735	18	59

The results of procedure of segmentation of Hubert are presented in tables 12, 13 and 14 for each of the same climate models (CCCmaCanESM2 model, MOHC-HadGEM2-ES model and MPI-M-MPI+ESM-LR model) with the associations S1-2-3, S1-2, S1-3, S2-3 of the climate stations.

The medium scenario (RCP4.5) indicates a downwards shift of 45% and 50% respectively (tables 12 and 14) for CCCmaCanESM2 and MPI-M-MPI+ESM-LR model) and an upwards shift of 60% (table 13).

For the high scenario (RCP8.5) an upwards shift is observed for all associations of gauges stations (between 16 and 66%). For the medium scenario, shift occurs around year 2073 (table 12), 2035 for (table 13) and 2015 (table 14). The shift appears between years 2039 and 2055 for scenario high.

Table 12: Results for CCCmaCanESM2 model (Using combination of station)

Canadian Centre for Climate Modelling and Analysis (CCCmaCanESM2)									
Station	RCP4.5					RCP8.5			
	Year	Year	Mean	Decreases/ increases	Standard deviation	Year	Year	Mean	Decreases/ increases
S1-2-3	2006	2075	509		1	2006	2055	393	
	2076	2090	380	-25	27	2056	2090	441	12
S1-2	2006	2073	113		16	2006	2056	108	
	2074	2090	52	-54	9	2057	2090	132	22
S1-3	2006	2073	350		31	2006	2055	331	
	2074	2090	171	-51	24	2056	2090	378	14
S2-3	2006	2073	311		18	2006	2055	293	
	2074	2090	149	-52	23	2056	2090	339	16

Table 13: Results for MOHC-HadGEM2-ES model (Using combination of station)

MOHC Met Office Hadley Centre, England									
Station	RCP4.5					RCP8.5			
	Year	Year	Mean	Decreases/ increases	Standard deviation	Year	Year	Mean	Decreases/ increases
S1-2-3	2006	2032	318		51	2006	2039	230	
	2033	2090	443	40	63	2040	2090	373	62
S1-2	2006	2041	74		28	2006	2039	78	
	2042	2090	136	84	30	2040	2090	152	94
S1-3	2006	2035	236		63	2006	2055	331	
	2036	2090	375	59	68	2056	2090	378	14
S2-3	2006	2035	203		57	2006	2039	100	
	2036	2090	330	63	61	2040	2090	193	93

Table 14: Results for MPI-M-MPI-ESM-LR model (Using combination of station)

MPI-M-MPI-ESM-LR									
Station	RCP4.5					RCP8.5			
	Year	Year	Mean	Decreases/ increases	Standard deviation	Year	Year	Mean	Decreases/ increases
S1-2-3	2006	2015	291		30	2006	2045	332	
	2016	2090	193	-34	24	2046	2090	399	20
S1-2	2006	2015	141		22	2006	2040	144	
	2016	2090	68	-52	15	2041	2090	175	21
S1-3	2006	2015	354		32	2006	2045	379	
	2016	2090	222	-37	27	2046	2090	456	20
S2-3	2006	2015	307		31	2006	2045	332	
	2016	2090	194	-37	25	2046	2090	399	20

3.3. Tests of flow for trend

Trends in annual time series for the period (2006-2090) have been checked for by using the Mann-Kendall test with the null hypothesis of no trend. When the null hypothesis is accepted, Sen's slope estimator has been applied to estimate the magnitude of the trend. For each of the three models, the two scenarios, medium,

RCP4.5 and high, (RCP8.5) are considered for the climate gauge stations considered separately, and in combination.

3.3.1 Mann-Kendall Test and Sen's slope estimator

The results of the Mann-Kendall test for trend are presented for the four stations considered separately (table 15) and in combination (table 16) for all scenario and for all climate models.

For the RCP4.5 scenario, null hypothesis of no trend H_0 is accepted for all stations and for all climate models, except for gauge station S3 for MPI-M-MPI-ESM-LR model. For RCP8.5 (tableau 15)

For the RCP8.5 scenario, the null hypothesis is rejected for all gauge stations and for all climate models except for S3 gauge station for MOHC-HadGEM2-ES model. (table 15). Sen's slope estimator indicates a linear trend for all stations and climate models where H_0 is accepted.

Table 15: Results of trends test

Model	CCCma-CanESM2				MOHC-HadGEM2-ES				MPI-M-MPI-ESM-LR				Scenario
	M-K	Sen's			M-K	Sen's			M-K	Sen's			
Stations	Z	H_0	SM	H_0	Z	H_0	SM	H_0	Z	H_0	SM	H_0	
S0	0.52	A	0.26		4.46	R	0.38		-0.47	A	-0.15		RCP4.5
S1	1.40	A	0.27		5.39	R	0.31		-0.52	A	-0.17		
S2	1.06	A	0.11		4.46	R	0.35		-1.50	A	-0.21		
S3	0.00	A	0.10		4.24	R	0.20		-2.99	R	-0.12	A	
S0	2.20	R	0.28		5.66	R	0.46		5.26	R	0.25		RCP8.5
S1	3.33	R	0.22		5.37	R	0.44		8.29	R	0.56	A	
S2	6.43	R	0.39		4.85	R	0.33		8.34	R	0.55	A	
S3	5.53	R	0.19	A	1.34	A	0.002		3.63	R	0.09	R	

Results of Mann-Kendall trend tests using associations of gauges stations are

presented in table 16. For the RCP4.5 scenario, null hypothesis H_0 is accepted for all stations when climate models CCCma-CanESM2 and MPI-M-MPI-ESM-LR are used to generate inputs to SWAT, except gauge station combination S2-3 for MPI-M-MPI-ESM-LR model (table 16). Null hypothesis of no trend is rejected for all combinations of rain gauges for MOHC-HadGEM2-ES model. Sen's slope estimator indicates a linear trend.

For the RCP8.5 scenario, the null hypothesis of no trend is rejected for all climate and for all combinations of rain gauges excepted combination S2-3 for the MOHC-HadGEM2-ES model and S1-S2-S3 combination for MPI-M-MPI-ESM-LR model. Sen's slope estimator indicates a linear trend except for S1-3 (MOHC-HadGEM2-ES model and MPI-M-MPI-ESM-LR model).

Table 16: Results of trends test (Using combination of station)

Model	CCCma-CanESM2				MOHC-HadGEM2-ES				MPI-M-MPI-ESM-LR			
	M-K		Sen's		M-K		Sen's		M-K		Sen's	
	Z	H_0	SM	H_0	Z	H_0	SM	H_0	Z	H_0	SM	H_0
Association of Stations												
S1-2-3	-0.03	A	-0.03		4.68	R	0.2	A	1.37	A	0.18	
S1-2	1.39	A	0.02		3.91	R	0.4	A	1.34	A	0.35	
S1-3	1.04	A	0.01		4.05	R	0.2	A	2.41	A	0.22	
S2-3	1.25	A	0.01		3.72	R	0.2	A	3.67	R	0.24	A
S1-2-3	5.72	R	0.15	A	5.04	R	0.3	A	1.56	A	0.28	
S1-2	5.77	R	0.23	A	4.66	R	0.4	A	2.98	R	0.38	A
S1-3	5.72	R	0.15	A	4.31	R	0	R	3.07	R	0.01	R
S2-3	6.70	R	0.18	A	0.40	A	0.4		4.03	R	0.37	A

M-K : Mann-Kendall; SM: Slope Medium;
 H_0 :Null hypothesis; Z: Test statistic.

4. Conclusion

The main objective of the present work is to check for shifts and trends in the time series of flow in the Bafing River Catchment (Senegal River) at the Bafing Makana stream gauge in the years 2006-2090. Three climate models (CCCmaCanESM2, MOHC-HadGEM2-ES and MPI-M-MPI-ESM-LR) have been run to generate climate data at four gauge stations in the Bafing Makana river basin. Two scenarios of CO2 emission have been chosen: medium (RCP4.5) and high (RCP8.5). The climate data generated at each gauge stations have been used as inputs in SWAT model, separately and in combination, to generate time series of stream flow at Bafing Makana stream gauge. Shifts have been checked for using Pettit test and Hubert's procedure for segmentation of time series. Mann Kendall test has been run to check for trend. When null hypothesis of no trend is rejected, Sen's slope estimator allows to verify whether trend is linear or not.

Shifts are detected in generated time series of flow by the two tests (Pettitt, Hubert's procedure of segmentation of time series) for all three climate models, for all scenarios (medium and high), and for all rain gauges, separately or in association. For the high scenario, an increasing shift in time series of generated runoff is observed pour all rain gauges, separately or in association, for all climate models, and for all time series, beginning between 2044 and 2055. For medium scenario, a decreasing shift in time series of generated runoff is noted for all rain gauges, separately or in association, for all-time series and for all climate models, except for MOHC-

HadGEM2-ES model. Shifts occurs between 2016 and 2073.

For the Mann Kendall trend test and for the RCP4.5 scenario, the null hypothesis of no trend is accepted for all the time series of generated runoff, for all climate models, for

all rain gauges taken separately or in combinations. For the RCP8.5 scenario, the null hypothesis of no trend is rejected for all the time series of generated runoff, for all climate models, for all rain gauges taken separately or in combinations. Sen's slope estimator generally indicates a linear trend.

IJSER

References

- [1] Juraj M. Cunderlik & Slobodan P. Simonovic (2005) Hydrological extremes in a southwestern Ontario river basin under future climate conditions/Extrêmes hydrologiques dans un bassin versant du sud-ouest de l'Ontario sous conditions climatiques futures, *Hydrological Sciences Journal*, 50:4, -654, DOI: [10.1623/hysj.2005.50.4.631](https://doi.org/10.1623/hysj.2005.50.4.631)
- [2] Antoine Hreiche , Wajdi Najem & Claude Bocquillon (2007). Hydrological impact simulations of climate change on Lebanese coastal rivers / Simulations des impacts hydrologiques du changement climatique sur les fleuves côtiers Libanais , *Hydrological Sciences Journal/Journal des Sciences Hydrologiques*, 52:6, 1119-1133, DOI: [10.1623/hysj.52.6.1119](https://doi.org/10.1623/hysj.52.6.1119).
- [3] Climate Change (2013). The Physical Science Basis Working Group I Contribution to the Fifth Assessment Report of the Intergovernmental Panel on Climate Change.
- [4] A.A Akinsanola^{1,2}, V.O Ajayi², A.T Adejare², O.E Adeyeri², I.E Gbode², K.O Ogunjobi², G Nikulin³, A.T. Abolude¹ (2017). Evaluation of rainfall simulations over West Africa in dynamically downscaled CMIP5 global circulation models. Article in *Theoretical and Applied Climatology* · March 2017. DOI [10.1007/s00704-017-2087-8](https://doi.org/10.1007/s00704-017-2087-8)
- [5] MARISA GOULDEN, DECLAN CONWAY & AURELIE PERSECHINO (2009). Adaptation to climate change in international river basins in Africa: a review / Adaptation au changement climatique dans les bassins fluviaux internationaux en Afrique: une revue, *Hydrological Sciences Journal*, 54:5, 805-828, DOI: [10.1623/hysj.54.5.805](https://doi.org/10.1623/hysj.54.5.805)
- [6] Changements Climatiques (2007). Un rapport du Groupe d'experts intergouvernemental sur l'évolution du climat. Bilan 2007 des changements climatiques : Rapport de synthèse
- [7] WHYCOS (2007). Renforcement des capacités nationales et régionales d'observation, transmission et traitement de données pour contribuer au développement durable du bassin du Fleuve Sénégal. Une composante du Système Mondial d'Observation du Cycle Hydrologique. Document de projet préliminaire Septembre 2007.
- [8] Ansoumana BODIAN (2011). Approche par modélisation pluie-débit de la connaissance régionale de la ressource en eau: Application au haut bassin du fleuve Sénégal. THESE DE DOCTORAT. p11
- [9] Isabelle Ceillier (2015). L'étude des impacts sur la biodiversité : intégration de la biodiversité dans l'évaluation environnementale des barrages sur les fleuves transfrontaliers d'Afrique de l'Ouest. Maîtrise en biologie université de SHERBROOKE. Juillet 2015. p18
- [10] Moussé Landing SANE^{1*}, Soussou SAMBOU¹, Didier Maria NDIONE¹, Issa LEYE¹, Seïdou KANE¹, Mamadou Lamine BADJI¹ (2017). Analyse et traitement des séries de débits annuels et mensuels sur le Fleuve Sénégal en amont du barrage de Manantali : cas des stations de Bafing Makana et DakkaSaidou.Rev. Ivoir. Sci. Technol., 30 (2017) 102 – 120. ISSN 1813-3290, <http://www.revist.ci>.
- [11] Didier Maria Ndione, Soussou Sambou, Moussé Landing Sané.,Seidou Kane, Issa Leye, Seni Tamba, Mohamed Talla Cissé (2017). Statistical analysis for assessing randomness, shift and trend in rainfall time series under climate variability

and change: Case of Senegal. Accepted for publication in Journal of Geoscience and Environnement protection, 2017. <http://www.script.org/journal/gep>. ISSN [ONLINE/2327-4344](http://www.script.org/journal/gep). ISSN: 23274336.

[12] Z. Yang^{1,2}, Y. Zhou², J. Wenninger^{2,3}, and S. Uhlenbrook^{2,3} (2012). The causes of flow regime shifts in the semi-arid Hailu River, Northwest China. Hydrol. Earth Syst. Sci., 16, 87–103, 2012. www.hydrol-earth-syst-sci.net/16/87/2012/ DOI:10.5194/hess-16-87-2012.

[13] Sebbar A, Badri W, Fougrach H, Hsaine M, Saloui A, 2011. _Etude de la variabilité du régime pluviométrique au Maroc septentrional (1935-2004). Sécheresse 22: Tires a_ part : A. Sebbar 139-48. doi : 10.1684/sec.2011.0313

[14] Milan Gocic*, Slavisa Trajkovic (2013). Analysis of changes in meteorological variables using Mann-Kendall and Sen's slop estimator statistical tests in Serbia. nal homepage: www.elsevier.com/locate/gloplacha. *Global and Planetary Change* 100 (2013) 172–182

[15] Huantian Xie, Dingfang Li, Lihua Xiong (2014). Exploring the ability of the Pettitt method for detecting change point by Monte Carlo simulation. Stoch Environ Res Risk Assess (2014) 28:1643–1655. DOI [10.1007/s00477-013-0814-y](https://doi.org/10.1007/s00477-013-0814-y)

[16] Arun Mondal^{1*}, Sananda Kundu¹, Anirban Mukhopadhyay² (2012). Rainfall trend analysis by mann-kendall test: a case study of north-eastern part of cuttack district, orissa. International Journal of Geology, Earth and Environmental Sciences ISSN: 2277-2081 (Online)An Online International Journal Available at

<http://www.cibtech.org/jgee.htm> 2012 Vol. 2 (1) January-April, pp.70-78/Mondal et al.

[17] Keredin Temam Siraj¹, Annisa Mohammed², Surendra Bam³, Solomon Addisu⁴. (2013). Long years comparative climate change trend analysis in terms of temperature, Coastal Andhra pradesh, India. Abhinav national monthly refereed journal of research in science & technology. Volume no.2, issue no.7. ISSN 2277-1174.

[18] Adamu Mustapha (2014). Detecting surface water quality trends using Mann-Kendall tests and Sen's slope estimates. *IJAIR* ISSN: 2278-7844. <https://www.researchgate.net/publication/235752471>.

[19] Cheikh Faye, Amadou Abdoul Sow et Jean Baptiste Ndong (2015). Étude des sécheresses pluviométriques et hydrologiques en Afrique tropicale : caractérisation et cartographie de la sécheresse par indices dans le haut bassin du fleuve Sénégal. p. 17-35 Volume 9 | 2015 : Varia 2015.

[20] Hashim Isam Jameel Al-Safi ^{a,b,*}, Priyantha Ranjan Sarukkalige ^a (2017). Assessment of future climate change impacts on hydrological behavior of Richmond River Catchment. Water Science and Engineering 2017, 10(3): 197-208. journal homepage: <http://www.waterjournal.cn>

[21] Hayhoe, K., J. Edmonds, R.E. Kopp, A.N. Le Grande, B.M. Sanderson, M.F. Wehner, and D.J. Wuebbles, 2017: Climate models, scenarios, and projections. In: *Climate Science Special Report: Fourth National Climate Assessment, Volume I* [Wuebbles, D.J., D.W. Fahey, K.A. Hibbard, D.J. Dokken, B.C. Stewart, and

T.K. Maycock (eds.)). U.S. Global Change Research Program, Washington, DC, USA, pp. 133-160, DOI : [10.7930/J0WH2N54](https://doi.org/10.7930/J0WH2N54).

[22] FRANZ RUBEL 1* and MARKUS KOTTEK2 (2010). Observed and projected climate shifts 1901–2100 depicted by world maps of the Köppen-Geiger climate classification. *Meteorologische Zeitschrift*, Vol. 19, No. 2, 135-141. DOI [10.1127/0941-2948/2010/0430](https://doi.org/10.1127/0941-2948/2010/0430)

[23] Intergovernmental Panel on Climate Change (2000). *A Special Report of IPCC Working Group III*. ISBN: 92-9169-113-5

[24] Stanley Ob Joseph (2018). Examining the impacts of projected precipitation changes on sugar beet yield in Eastern England. A thesis submitted for the degree of Doctor of Philosophy. p25

[25] Ansoumana Bodian 1,*, Alain Dezetter 2, Lamine Diop 3, Abdoulaye Deme 4, Koffi Djaman 5 and Aliou Diop 6 (2018). Future Climate Change Impacts on Streamflows of Two Main West Africa River Basins: Senegal and Gambia. *Hydrology* 2018, 5, 21; www.mdpi.com/journal/hydrology. DOI: [10.3390/hydrology5010021](https://doi.org/10.3390/hydrology5010021)

[26] R. A. Betts^{1,2}, N. Golding¹, P. Gonzalez³, J. Gornall¹, R. Kahana¹, G. Kay¹, L. Mitchell¹, and A. Wiltshire¹ (2015). Climate and land use change impacts on global terrestrial ecosystems and river flows in the HadGEM2-ES Earth system model using the representative concentration pathways. *Biogeosciences*, 12, 1317–1338, 2015. www.biogeosciences.net/12/1317/2015/. doi:10.5194/bg-12-1317-2015.

[27] AMANDA S. MATHYS¹, NICHOLAS C. COOPS¹ and RICHARD H. WARING² (2015). An ecoregion assessment of projected tree species vulnerabilities in western North America

through the 21st century. *Global Change Biology* (2016), DOI: [10.1111/gcb.13440](https://doi.org/10.1111/gcb.13440).

[28] Kaustubh Salvi¹ · Subimal Ghosh^{1,2} · Auroop R. Ganguly^{2,3} (2015). Credibility of statistical downscaling under nonstationary climate. Springer-Verlag Berlin Heidelberg 2015. DOI [10.1007/s00382-015-2688-9](https://doi.org/10.1007/s00382-015-2688-9)

[29] P. HUBERT, E. SERVAT, J.-E. PATUREL, B. KOUAME, H. BENDJOUDI, J.-P. CARBONNEL, H. LUBES-NIEL (1998). La procédure de segmentation, dix ans après. *Water Resources Variability in Africa during the XXth Century* (proceedings of the Abidjan'98 Conference 267 held at Abidjan, Côte d'Ivoire. November (1998). IAHS Publ. no. 252, 1998.

[30] J. E. PATUREL, E. SERVAT, M. O. DELATTRE, Analyse de séries pluviométriques de longue durée en Afrique de l'Ouest et Centrale non sahélienne dans un contexte de variabilité climatique. *Hydrological Sciences-Journal des Sciences Hydrologiques*, 43 (6) (December 1998)

[31] S. Harrigan¹, C. Murphy¹, J. Hall², R. L. Wilby³, and J. Sweeney¹ (2014). Attribution of detected changes in streamflow using multiple working hypotheses. *Hydrol. Earth Syst. Sci.*, 18, 1935–1952, 2014. www.hydrol-earth-syst-sci.net/18/1935/2014/. doi :10.5194/hess-18-1935-2014

[32] Donald H. Burn, Juraj M. Cunderlik & Alain Pietroniro (2004) Hydrological trends and variability in the Liard River basin / Tendances hydrologiques et variabilité dans le bassin de la rivière Liard, *Hydrological Sciences Journal*, 49:1, 53-67, DOI: [10.1623/hysj.49.1.53.53994](https://doi.org/10.1623/hysj.49.1.53.53994)

[33] M. G. KENDALL, Rank Correlation Methods, 4th ed., Charles Griffin: London, (1975).

[34] Collaud Coen, M., E. Weingartner, S. Nyeki, J. Cozic, S. Henning, B. Verheggen, R. Gehrig, and U. Baltensperger (2007), Long-term trend analysis of aerosol variables at the high-alpine site Jungfraujoch, J. Geophys. Res., 112, D13213, DOI:10.1029/2006JD007995.

[35] Hossein Tabari, Meron Teferi Taye, Patrick Willems (2015). Évaluation statistique de l'évolution des précipitations dans le bassin supérieur du Nil Bleu.

Recherche environnementale stochastique et évaluation des risques Octobre 2015, Volume 29, Numéro 7, pp 1751–1761

[36] Fati Aziz†* and Emmanuel Obuobie‡ (2017). Trend analysis in observed and projected precipitation and mean temperature over the Black Volta Basin, West Africa. International Journal of Current Engineering and Technology E-ISSN 2277 – 4106, P-ISSN 2347 – 5161. Vol.7, No.4 (Aug 2017).

IJSER